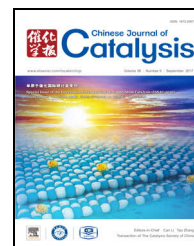


available at [www.sciencedirect.com](http://www.sciencedirect.com)journal homepage: [www.elsevier.com/locate/chnjc](http://www.elsevier.com/locate/chnjc)

Article (Special Issue of the International Symposium on Single-Atom Catalysis (ISSAC-2016))

# Effect of the degree of dispersion of Pt over MgAl<sub>2</sub>O<sub>4</sub> on the catalytic hydrogenation of benzaldehyde

Feng Yan <sup>a,b</sup>, Caixian Zhao <sup>a</sup>, Lanhua Yi <sup>a,\*</sup>, Jingcai Zhang <sup>b</sup>, Binghui Ge <sup>c</sup>, Tao Zhang <sup>b</sup>, Weizhen Li <sup>b,#</sup><sup>a</sup> Key Laboratory of Environmentally Friendly Chemistry and Applications of Ministry of Education, School of Chemistry, Xiangtan University, Xiangtan 411105, Hunan, China<sup>b</sup> State Key Laboratory of Catalysis, Dalian Institute of Chemical Physics, Chinese Academy of Sciences, Dalian 116023, Liaoning, China<sup>c</sup> Beijing National Laboratory for Condensed Matter Physics, Institute of Physics, Chinese Academy of Sciences, Beijing 100190, China

## ARTICLE INFO

## Article history:

Received 14 February 2017

Accepted 15 March 2017

Published 5 September 2017

## Keywords:

Platinum

MgAl<sub>2</sub>O<sub>4</sub> spinel

Single-atom catalyst

Selective hydrogenation

Benzaldehyde

Benzyl alcohol

## ABSTRACT

One of the central tasks in the field of heterogeneous catalysis is to establish structure-function relationships for these catalysts, especially for precious metals dispersed on the sub-nanometer scale. Here, we report the preparation of MgAl<sub>2</sub>O<sub>4</sub>-supported Pt nanoparticles, amorphous aggregates and single atoms, and evaluate their ability to catalyze the hydrogenation of benzaldehyde. The Pt species were characterized by N<sub>2</sub> adsorption, X-ray diffraction (XRD), aberration-corrected transmission electron microscopy (ACTEM), CO chemisorption and *in situ* Fourier transform infrared spectroscopy of the chemisorbed CO, as well as by inductively coupled plasma atomic emission spectroscopy. They existed as isolated or neighboring single atoms on the MgAl<sub>2</sub>O<sub>4</sub> support, and formed amorphous Pt aggregates and then nanocrystallites with increased Pt loading. On the MgAl<sub>2</sub>O<sub>4</sub> support, single Pt atoms were highly active in the selective catalytic hydrogenation of benzaldehyde to benzyl alcohol. The terrace atoms of the Pt particles were more active but less selective; this was presumably due to their ability to form bridged carbonyl adsorbates. The MgAl<sub>2</sub>O<sub>4</sub>-supported single-atom Pt catalyst is a novel catalyst with a high precious atom efficiency and excellent catalytic hydrogenation ability and selectivity.

© 2017, Dalian Institute of Chemical Physics, Chinese Academy of Sciences.

Published by Elsevier B.V. All rights reserved.

## 1. Introduction

Supported noble metal catalysts are widely used in the selective hydrogenation of organic compounds to give valuable derivatives [1]. Selective catalytic hydrogenation of benzaldehyde (BzH) is a green route to the production of benzyl alcohol (BA), which is an important feedstock for the synthesis of vitamins, pharmaceuticals, pesticides, fragrances and various es-

ters [2]. Hydrogenation of BzH can give various products by either partial or complete reduction of the carbonyl group and/or benzene ring, and thus serves as a model reaction for probing the catalytic hydrogenation ability of specific catalysts [3–5]. Platinum and ruthenium catalysts tend to be more chemoselective for reduction of the carbonyl group than reduction of the C=C bonds, and their main drawback is further hydrodeoxygenation of BA into toluene (TOL) [5,6]. Because only

\* Corresponding author. Tel: +86-731-58293719; Fax: +86-731-58292477; E-mail: yilanhua@xtu.edu.cn

# Corresponding author. Tel: +86-411-84379738; Fax: +86-411-84685940; E-mail: weizhenli@dicp.ac.cn

This work was supported by the National Natural Science Foundation of China (21403213, 21673226, 21376236, U1462121), the “Hundred Talents Programme” of the Chinese Academy of Sciences, and National Key R&amp;D Program of China (2016YFA0202801), and the “Strategic Priority Research Program” of the Chinese Academy of Sciences (XDB17020100), Department of Science and Technology of Liaoning province under contract of 2015020086-101, and the Natural Science Foundation of Hunan Province (2016JJ2128).

DOI: 10.1016/S1872-2067(17)62815-8 | <http://www.sciencedirect.com/science/journal/18722067> | Chin. J. Catal., Vol. 38, No. 9, September 2017

surface metal atoms are accessible to reactants and can act as active sites, the metal catalysts are dispersed as very small particles on support materials to give a high specific surface area. Unlike homogeneous catalysts, which are uniform complexes with defined central metal ions and ligands, supported metal particles usually contain exposed atoms in various environments, and the local coordination environments are not adequately characterized on the atomic level [7,8]. In fact, the structures of the surface metals in a supported catalyst are complicated because of the various sizes of the metal particles and their varied locations on the support material. Each site coexisting on a metal particle provides its own activity and selectivity profile, and thus varies the overall catalytic performance according to its relative size and contribution.

Particle size diversity in supported metal catalysts is a major parameter affecting their catalytic performance. Most commercial supported metal catalysts are prepared by a conventional impregnation method, during which the precious metal atoms may form dissolved cations, cations adsorbed on the support, or highly dispersed or aggregated oxide and/or metallic species and/or particles. The metal particles and their distributions are generally characterized by high resolution transmission electron microscopy (HRTEM), and thus the relationship between the catalyst structure and the catalytic performance can be established. However, characterization of the catalysts with spherical aberration-corrected transmission electron microscopy (ACTEM), a new technique, has shown that, besides metal particles, single-atom metal species are also common, irrespective of the support material [9–13]. Such single-atom metal species are active structures in many reactions and, in some cases, even more active than their nanoparticle counterparts. They have therefore become the subject of research in the new field of “single-atom catalysis” [13–21]. Thus, it is necessary to reconsider the active sites of supported metal catalysts and re-evaluate their relative catalytic contributions. Among the reported Pt catalysts that contain single-atom Pt species, Pt/MgAl<sub>2</sub>O<sub>4</sub>, with proper modification, is particularly suitable as a model catalyst owing to its superior stability and activity [11,22].

In this work, we report the preparation of MgAl<sub>2</sub>O<sub>4</sub> spinel-supported single-atom to nano-sized Pt catalysts and their catalytic performance in the catalytic hydrogenation of BzH. We characterized the Pt/MgAl<sub>2</sub>O<sub>4</sub> catalysts using BET, X-ray diffraction (XRD), ACTEM, inductively coupled plasma atomic emission spectroscopy (ICP-AES), CO chemisorption and Fourier transform infrared (FTIR) spectroscopy of the adsorbed CO species, and analyzed the relationship between the catalytic performance and the catalyst structure.

## 2. Experimental

### 2.1. Catalyst preparation

MgAl<sub>2</sub>O<sub>4</sub> spinel support material was prepared by hydrolysis of aluminum isopropoxide with magnesium nitrate hexahydrate in ethanol, followed by calcination of the precipitates in ambient air at 800 °C for 5 h with a heating rate of 2 °C/min.

MgAl<sub>2</sub>O<sub>4</sub>-supported Pt catalysts were prepared by soaking 10 g of the MgAl<sub>2</sub>O<sub>4</sub> support powders in 200 mL of an aqueous solution of chloroplatinic acid hexahydrate (Pt content >37.5%, Tianjin Fengchuan Chemical Reagent Technologies Co., Ltd.) for 10 h under magnetic stirring. Appropriate amounts of Pt were used to give nominal loadings of 0.2 wt%, 0.5 wt% and 1 wt%. The powders were separated by filtration and washed three times with deionized water. The impregnated samples were dried at 60 °C overnight, calcined at 500 °C for 5 h and finally reduced at 300 °C in H<sub>2</sub> for 2 h. The catalysts are denoted 0.2Pt/MgAl<sub>2</sub>O<sub>4</sub>, 0.5Pt/MgAl<sub>2</sub>O<sub>4</sub> and 1Pt/MgAl<sub>2</sub>O<sub>4</sub>, and the actual Pt loadings were determined by ICP-AES to be 0.19 wt%, 0.47 wt% and 0.92 wt%, respectively.

### 2.2. Catalyst characterization

Surface areas were measured on a Micromeritics ASAP 2010 apparatus using N<sub>2</sub> adsorption isotherms and Brunauer-Emmett-Teller (BET) analysis methods. All samples were degassed under vacuum at 300 °C for 5 h before the adsorption measurements. The content of Pt in the catalysts was measured on an ICP-AES 7300DV instrument. All samples were dissolved in *aqua regia* by microwave-assisted digestion at 900 W for 1 h. XRD patterns were recorded on a PW3040/60 X'Pert PRO (PANalytical) diffractometer equipped with a Cu K $\alpha$  radiation source ( $\lambda = 0.15432$  nm) operating at 40 kV and 40 mA. High-angle annular dark field scanning transmission electron microscopy (HAADF-STEM) images were obtained on a JEOL JEM-ARM200F microscope equipped with a CEOS probe corrector, with a guaranteed resolution of 0.08 nm. TEM specimens were prepared by depositing a suspension of the powdered sample on a lacey carbon-coated copper grid. Pt dispersions were measured by pulse adsorption of CO on a Micromeritics AutoChem II 2920 automated characterization system at 50 °C. Approximately 200 mg of the sample was loaded into a U-shaped quartz tube and heated to 300 °C for 30 min under pure H<sub>2</sub> (30 mL/min) and then cooled to 50 °C in pure He (30 mL/min). CO pulses (10%CO-90%He) were introduced by switching a six-way sampling valve. Pt dispersions were estimated by assuming the adsorption stoichiometry of CO to Pt to be equal to 1. *In situ* diffuse reflectance FTIR spectra of the adsorbed CO species were acquired with a Bruker Equinox 55 spectrometer equipped with a mercury cadmium telluride (MCT) detector at a spectral resolution of 4 cm<sup>-1</sup> and with 32 scans. The sample powders were loaded into the IR cell, pretreated in pure H<sub>2</sub> (6 mL/min) at 300 °C for 1 h at a heating rate of 10 °C/min and then cooled to 50 °C in He (30 mL/min). The background spectrum was recorded under this condition. Then, CO/He (1 vol%, 30 mL/min) was introduced for 30 min and the sample was flushed with pure He (30 mL/min) before the spectra of chemisorbed CO were recorded.

### 2.3. Hydrogenation of benzaldehyde

Liquid-phase hydrogenation of BzH was conducted in a 10-mL Teflon-lined stainless steel autoclave reactor. In a typical hydrogenation reaction, 20 mg of the Pt/MgAl<sub>2</sub>O<sub>4</sub> catalyst (or

**Table 1**  
Characteristics of the Pt/MgAl<sub>2</sub>O<sub>4</sub> catalysts.

Catalyst	$S_{\text{BET}}$ (m <sup>2</sup> /g)	Pore size (nm)	Pore volume (cm <sup>3</sup> /g)	Pt loading (wt%)	Pt dispersion <sup>a</sup> (%)
0.2Pt/MgAl <sub>2</sub> O <sub>4</sub>	129.8	7.1	0.46	0.19	92.5
0.5Pt/MgAl <sub>2</sub> O <sub>4</sub>	124.6	7.4	0.46	0.47	63.9
1Pt/MgAl <sub>2</sub> O <sub>4</sub>	126.7	7.5	0.48	0.92	53.2

<sup>a</sup> Determined by CO chemisorption at 50 °C with assuming CO/Pt = 1.

1 μmol equivalent of Pt) was suspended in 5 mL ethanol containing 100 μL BzH (>97%, AIKE Reagent, ~1 mmol). After the air was replaced three times with H<sub>2</sub>, the autoclave was charged with H<sub>2</sub> (1.0 MPa) and maintained at various temperatures for various time under vigorous magnetic stirring. The absence of external diffusion limitations was verified by performing the reaction under various stirring rates in preliminary experiments. After the reaction, the autoclave was quenched with cold water. A reusability test was conducted with the 0.2Pt/MgAl<sub>2</sub>O<sub>4</sub> catalyst, whereby the used catalyst was collected and recovered by filtration and washing with ethanol. The shortfall in the recovered catalyst was replenished with catalysts from other reactors that had undergone the same number of runs. The products were analyzed by gas chromatography (7890B, Agilent Technologies) using an HP-INNOWAX capillary column (30 m × 0.32 mm, Agilent Technologies) and a flame ionization detector.

### 3. Results and discussion

#### 3.1. Catalyst structure determination

The physico-chemical characteristics of the three Pt/MgAl<sub>2</sub>O<sub>4</sub> catalysts are presented in Table 1. The surface areas, pore sizes and pore volumes of all three catalysts were 124–130 m<sup>2</sup>/g, 7.1–7.5 nm and 0.46–0.48 cm<sup>3</sup>/g, respectively, which indicates that the textural properties of the MgAl<sub>2</sub>O<sub>4</sub> support materials changed little during the catalyst preparation process. The Pt loadings were accurately determined by ICP-AES to be 0.19 wt%, 0.47 wt% and 0.92 wt% for 0.2Pt/MgAl<sub>2</sub>O<sub>4</sub>, 0.5Pt/MgAl<sub>2</sub>O<sub>4</sub> and 1Pt/MgAl<sub>2</sub>O<sub>4</sub>, respectively. The Pt dispersions were respectively estimated as 92.5%, 63.9% and 53.2% using CO chemisorption. The XRD patterns

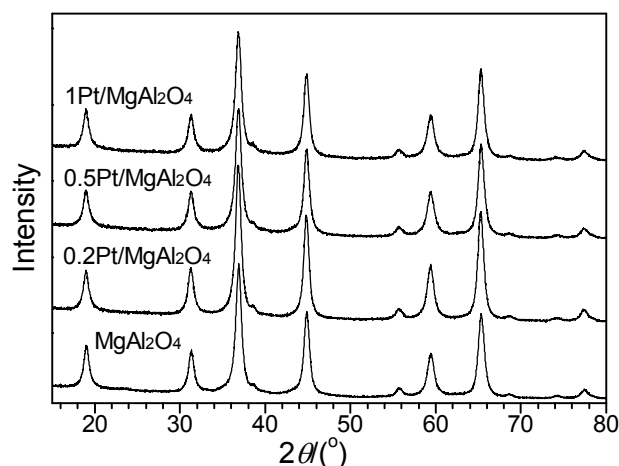


**Fig. 1.** XRD patterns for the Pt/MgAl<sub>2</sub>O<sub>4</sub> catalysts and the MgAl<sub>2</sub>O<sub>4</sub> support material.

shown in Fig. 1 for the Pt/MgAl<sub>2</sub>O<sub>4</sub> catalysts are identical to that of the MgAl<sub>2</sub>O<sub>4</sub> support, which appears as a pure spinel crystal phase. The lack of detectable diffractions for Pt indicates that the mean Pt crystallite sizes are below the detection limit of XRD (~3 nm) in all samples. Representative HAADF-STEM images show that 0.2Pt/MgAl<sub>2</sub>O<sub>4</sub> presents a large amount of single-atom Pt species as isolated bright dots on the MgAl<sub>2</sub>O<sub>4</sub> substrate, and very occasionally Pt aggregates (Fig. 2(a)). Notably, the Pt aggregates appear to be amorphous, not crystallites with clear edges, which suggests that they do not contain enough atoms to form well-defined crystalline particles. Interestingly, 0.5Pt/MgAl<sub>2</sub>O<sub>4</sub> displays many neighboring single Pt atoms in addition to the highly isolated Pt atoms and amorphous aggregates (Fig. 2(b)). This is reasonable because the surface density of Pt atoms on the MgAl<sub>2</sub>O<sub>4</sub> substrate increases with increased Pt loading. In the 1Pt/MgAl<sub>2</sub>O<sub>4</sub> sample, the amorphous Pt aggregates become dominant, and are accompanied by occasional isolated single Pt atoms and rare well-defined Pt crystallites of less than 2 nm (Fig. 2(c)). Clearly, with increased Pt loading, the packing of the Pt atoms on the MgAl<sub>2</sub>O<sub>4</sub> surface becomes denser, and presents various Pt species, for example, isolated single Pt atoms, single-layered neighboring Pt atoms, amorphous aggregates and well-defined crystalline particles, depending on the local Pt atom density. These species include almost all possible transition forms, and thus illustrate the process for the

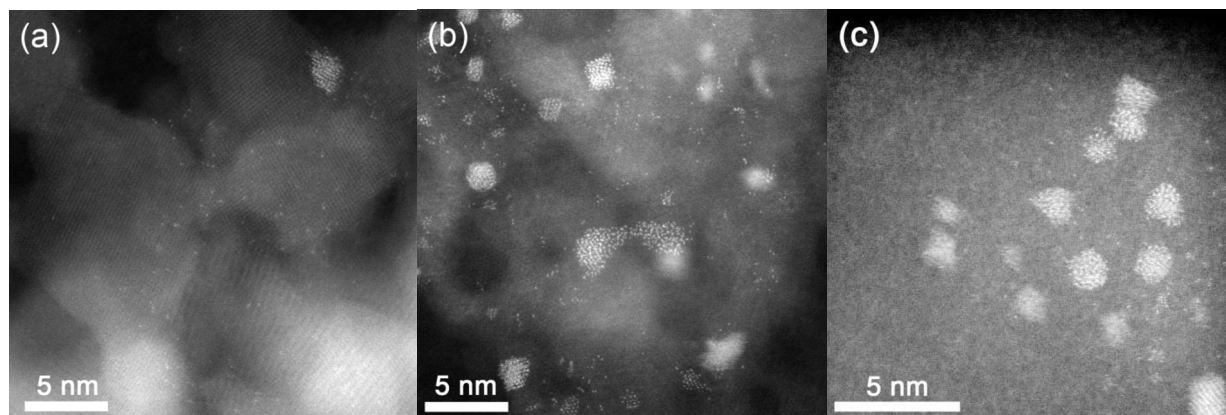


**Fig. 2.** HAADF-STEM images for the 0.2Pt/MgAl<sub>2</sub>O<sub>4</sub> (a), 0.5Pt/MgAl<sub>2</sub>O<sub>4</sub> (b), and 1Pt/MgAl<sub>2</sub>O<sub>4</sub> (c) catalysts.

formation of metal crystallites on a support substrate in slow motion. Similar processes are expected, and indeed evident albeit in a much faster mode, for Pt and other noble metals dispersed on various support materials [9,10]. The Pt/MgAl<sub>2</sub>O<sub>4</sub> catalysts retain much more of the single-atom and amorphous aggregate characteristics than conventional supported metal catalysts; this is presumably due to the markedly stronger metal/support interaction in this system.

*In situ* FTIR spectroscopy of CO adsorbed on the Pt/MgAl<sub>2</sub>O<sub>4</sub> catalysts was used to probe the possible differences in the coordination environments of the accessible Pt atoms in various Pt species. As shown in Fig. 3, 1Pt/MgAl<sub>2</sub>O<sub>4</sub> presents four bands centered at 1820, 2030, 2073 and 2080 cm<sup>-1</sup>. The 0.5Pt/MgAl<sub>2</sub>O<sub>4</sub> catalyst displays two distinct bands centered at 1820 and 2073 cm<sup>-1</sup>, and a shoulder peak at approximately 2030 cm<sup>-1</sup>. However, 0.2Pt/MgAl<sub>2</sub>O<sub>4</sub> presents only a broad asymmetric band at 2065 cm<sup>-1</sup> and a small band at 1820 cm<sup>-1</sup>. According to empirical interpretations of the FTIR spectra of CO adsorbed on metals, bands in the low frequency range (1730–1900 cm<sup>-1</sup>) are usually assigned to bridged carbonyl species on neighboring metal atoms, whereas those in the high frequency range (1950–2100 cm<sup>-1</sup>) are assigned to linear carbonyl species on metals in various chemical environments [23,24]. Thus, based on this expected blue shift in the stretching frequency with increasing coordination degree (or metallic nature) of the Pt atom, the CO adsorption bands at 2065, 2073 and 2080 cm<sup>-1</sup> in the spectra described above were assigned to the collective oscillation of CO linearly adsorbed on the single Pt atoms, amorphous aggregates and crystallites. The band at 2030 cm<sup>-1</sup> was assigned to the collective oscillation of CO linearly adsorbed on the highly under-coordinated Pt on the edges or corners of the Pt crystallites [23]. The CO adsorption band at 1820 cm<sup>-1</sup> was assigned to the bridged CO species adsorbed on the terraces of the well-defined Pt crystallites [24]. On the basis of the relative band areas of the linear and bridged carbonyl species, it is clear that the number of terrace atoms markedly increases with Pt loading, which is in line with the observed increase in the density of Pt crystallites shown in Fig. 2.

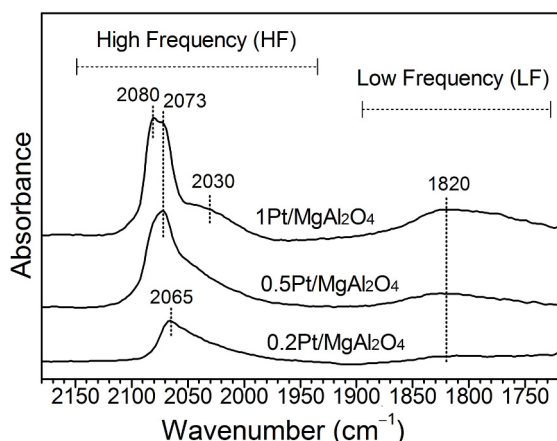


**Fig. 3.** FT-IR spectra of CO adsorbed on the Pt/MgAl<sub>2</sub>O<sub>4</sub> catalysts at 50 °C. The high-frequency vibrational mode was assigned to CO linearly bound to Pt atoms in various chemical environments, and the low-frequency mode was assigned to bridged carbonyl species on neighboring Pt atoms on crystallite.

### 3.2. Evaluation of the catalytic performance

To explore the catalytic hydrogenation ability of the Pt/MgAl<sub>2</sub>O<sub>4</sub> catalysts, we conducted hydrogenation of BzH under various reaction conditions and 100% BzH conversion. As shown in Table 2, three products were obtained: BA, TOL and benzaldehyde diethyl acetal (BDA). As illustrated in Scheme 1, BA is produced by the selective hydrogenation of BzH, TOL is generated through hydrodeoxygenation of the carbon-oxygen bonds in BzH or BA, and BDA is formed by aldol condensation of BzH and the ethanol solvent. The results are displayed as the molar compositions of the products. Under mild reaction conditions, with a temperature of 60 °C, H<sub>2</sub> pressure of 1.0 MPa and time of 4 h, the 0.2Pt/MgAl<sub>2</sub>O<sub>4</sub>, 0.5Pt/MgAl<sub>2</sub>O<sub>4</sub> and 1Pt/MgAl<sub>2</sub>O<sub>4</sub> catalysts were highly active in the selective hydrogenation of BzH to BA, but much less active in the hydrodeoxygenation to TOL. The high selectivity for BA decreased slightly from 99.4% to 99.1% and 99.0% and the low selectivity for TOL increased slightly from 0.4% to 0.6% and 0.7% as the Pt loading was increased from 0.2 wt% to 0.5 wt% and 1 wt%, respectively. BDA was detected with similar selectivities and yields of (0.2–0.3)% for all three catalysts. A comparable yield of BDA was also obtained for 1Pt/MgAl<sub>2</sub>O<sub>4</sub> under similar reaction conditions when the atmosphere was changed to N<sub>2</sub>. This suggests that the formation of BDA is a parallel side reaction with a much slower rate. When the reaction temperature was elevated to 100 and 150 °C, the 0.2Pt/MgAl<sub>2</sub>O<sub>4</sub> catalyst presented a slightly decreased selectivity for BA (98.8% and

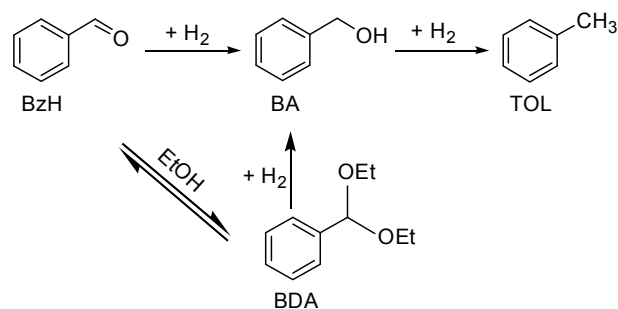
**Table 2**

Catalytic results for benzaldehyde hydrogenation over the Pt/MgAl<sub>2</sub>O<sub>4</sub> catalysts at various temperatures.

Catalyst	Temperature (°C)	Conversion (%)	Product distribution (%)		
			BA	TOL	BDA
0.2Pt/MgAl <sub>2</sub> O <sub>4</sub>	60	100	99.4	0.4	0.2
	100	100	98.8	0.5	0.7
	150	100	97.9	0.4	1.7
0.5Pt/MgAl <sub>2</sub> O <sub>4</sub>	60	100	99.1	0.6	0.3
	100	100	98.4	0.8	0.8
	150	100	96.4	1.9	1.7
1Pt/MgAl <sub>2</sub> O <sub>4</sub>	60	100	99.0	0.7	0.3
	100	100	95.4	3.9	0.7
	150	100	93.1	5.0	1.9
1Pt/MgAl <sub>2</sub> O <sub>4</sub> <sup>#</sup>	60	1.5	37.3	0	62.7

Reaction conditions: 20.0 mg catalyst, 100 μL BAL (~1 mmol), 5.0 mL ethanol as solvent, 1.0 MPa of H<sub>2</sub>, 4 h.

<sup>#</sup> Reaction under similar conditions except the atmosphere is N<sub>2</sub>.



**Scheme 1.** Possible reaction pathways of benzaldehyde hydrogenation over Pt/MgAl<sub>2</sub>O<sub>4</sub> catalysts in ethanol medium.

97.9%) and increased selectivity for BDA (0.7% and 1.7%), whereas the selectivity for TOL was almost unchanged (0.5% and 0.4%). The 0.5Pt/MgAl<sub>2</sub>O<sub>4</sub> catalyst, however, showed a notable increase in the selectivity for TOL (to 0.8% and 1.9%) and a decrease in the selectivity for BA (to 98.4% and 96.4%) in reactions at 100 and 150 °C. Similarly, 1Pt/MgAl<sub>2</sub>O<sub>4</sub> also showed increased selectivity for TOL (to 3.9% and 5.0%) and decreased selectivity for BA (to 95.4% and 93.1%). The selectivities for BDA appear to be comparable for all temperatures and catalysts. Through hydrogenation of BzH at 100% conversion and over a wide temperature range, the catalytic hydrogenation ability of the Pt/MgAl<sub>2</sub>O<sub>4</sub> catalysts was evaluated. Selective hydrogenation of BzH to give BA is the predominant reaction over all three Pt/MgAl<sub>2</sub>O<sub>4</sub> catalysts. Hydrodeoxygenation of the carbon-oxygen bonds in BzH or BA to give TOL is negligible for 0.2Pt/MgAl<sub>2</sub>O<sub>4</sub>, but becomes meaningful when the Pt loading is increased to 0.5 wt% and above.

The catalytic activities of the Pt/MgAl<sub>2</sub>O<sub>4</sub> catalysts were further investigated at various temperatures and BzH conversions by using catalysts containing similar amounts of Pt (~1 μmol). As displayed in Table 3, 0.2Pt/MgAl<sub>2</sub>O<sub>4</sub> catalyzed the hydrogenation of BzH at temperatures as low as 20 °C with 1.0 MPa of H<sub>2</sub>. Under these conditions, the BzH conversion was 55.3% after 15 h, with BA, TOL and BDA selectivities of 98.8%, 0 and 1.2%, respectively. When the catalytic activity was normalized to the total number of Pt atoms and surface Pt atoms determined by CO chemisorption experiments, the catalytic reaction rate and turnover frequency (TOF) were calculated to be 284 mol/(mol·h) and 307 h<sup>-1</sup>, respectively. After reaction at 40 °C for 2 h, the BzH conversion reached 30.1% and the BA, TOL and BDA selectivities were 99.3%, 0 and 0.7%, respectively. Additionally, the catalytic reaction rate and TOF increased to 1160 mol/(mol·h) and 1254 h<sup>-1</sup>, respectively. After reaction at 60 °C for 0.3, 1 and 2 h, the BzH conversions increased from 22.5% to 53.6% and 94.9%, and the calculated rate and TOF decreased from 3430 to 2700 and 2388 mol/(mol·h) and from 3708 to 2919 and 2582 h<sup>-1</sup>, respectively. For 1Pt/MgAl<sub>2</sub>O<sub>4</sub>, after reaction at 60 °C for 0.3, 1 and 2 h, the BzH conversions increased from 19.4% to 45.9% and 90.1%, and the calculated reaction rate and TOF decreased from 3055 to 2386 and 2072 mol/(mol·h) and from 5472 to 4485 and 3895 h<sup>-1</sup>, respectively. The calculated reaction rates and TOFs are clearly related to the reaction time, although, according to the rate equation, the intrinsic factors affecting these parameters are the instantaneous concentrations of the reactants and products [25]. Thus,

the catalytic activities that were obtained at the same temperature and with similar BzH conversions were compared among the Pt/MgAl<sub>2</sub>O<sub>4</sub> catalysts. At BzH conversions of approximately 20%, the reaction rates for 0.2Pt/MgAl<sub>2</sub>O<sub>4</sub> and 1Pt/MgAl<sub>2</sub>O<sub>4</sub> were 3430 and 3055 mol/(mol·h), respectively, and the TOFs were 3708 and 5742 h<sup>-1</sup>, respectively. The inverse change in the mass specific rates and TOFs suggests that the surface Pt atoms on the Pt nanocrystallites are highly active and can partially compensate for the loss of accessible Pt atoms inside the particles. It is notable that the selectivity of 1Pt/MgAl<sub>2</sub>O<sub>4</sub> for BDA at 60 °C and low BzH conversions reached (10–20)%, and that BDA was eventually almost completely converted to BA by catalytic hydrogenation. This supports the reaction pathways illustrated in Scheme 1. A previously described Pt/MgAl<sub>2</sub>O<sub>4</sub> catalyst prepared by colloidal deposition has been shown to have a TOF of 56 h<sup>-1</sup> at 40 °C and 0.1 MPa of H<sub>2</sub> [5]. A Pt/dendrimer core/shell catalyst has been reported to have a TOF of 91 h<sup>-1</sup> under the same conditions [26], and a Pt/TiO<sub>2</sub> catalyst displays a TOF of 2448 h<sup>-1</sup> at 80 °C and 0.1 MPa of H<sub>2</sub> [27]. Clearly, all of the Pt/MgAl<sub>2</sub>O<sub>4</sub> catalysts in this work are considerably more active under similar reaction conditions, irrespective of Pt loading and dispersion degree; this is presumably due to the strong interaction between the Pt species and the MgAl<sub>2</sub>O<sub>4</sub> spinel support.

Because 0.2Pt/MgAl<sub>2</sub>O<sub>4</sub> represents a novel catalyst and has the highest Pt availability and BA selectivity, we performed recycling experiments and evaluated the reusability of the catalyst. In these experiments, we were more interested in the stability of the catalyst and the BA selectivity than in the kinetic activity, so we conducted the reaction under conditions that gave total BzH conversion. As shown in Fig. 4, the BzH conversions remained at 100% and the BA selectivity at about 99.5% over at least six runs. Even though the 0.2Pt/MgAl<sub>2</sub>O<sub>4</sub> catalyst was not able to provide high kinetic activity, the excellent stability of this catalyst in terms of BA selectivity was demonstrated, and indicates that the highly dispersed nature of the Pt species was unchanged during the recycling experiments.

### 3.3. Relationship between catalyst structure and catalytic function

The dispersion of Pt on an MgAl<sub>2</sub>O<sub>4</sub> spinel support can result in the formation of isolated or neighboring single Pt atoms, amorphous Pt aggregates and well-defined crystalline particles; the species formed depend on the local Pt atom density. With a

**Table 3**

The catalytic selectivities and activities of the Pt/MgAl<sub>2</sub>O<sub>4</sub> catalysts for benzaldehyde hydrogenation at low conversions.

Catalyst	Temperature (°C)	Time (h)	Conversion (%)	Product distribution (%)			Rate (mol/(mol·h))	TOF (h <sup>-1</sup> )
				BA	TOL	BDA		
0.2Pt/MgAl <sub>2</sub> O <sub>4</sub>	20	15	55.3	98.8	0	1.2	284	307
	40	2	30.1	99.3	0	0.7	1160	1254
	60	0.3	22.5	97.7	1.1	1.2	3430	3708
	60	1	53.6	98.6	1.0	0.4	2700	2919
	60	2	94.9	99.5	0.4	0.1	2388	2582
1Pt/MgAl <sub>2</sub> O <sub>4</sub>	60	0.3	19.4	79.1	1.1	19.9	3055	5742
	60	1	45.9	89.5	1.4	9.1	2386	4485
	60	2	90.1	87.6	1.7	10.7	2072	3895

Reaction conditions: catalyst with similar amount of Pt (~0.2 μmol), 100 μL BAL (~1 mmol), 5.0 mL ethanol as solvent, 1.0 MPa of H<sub>2</sub>.

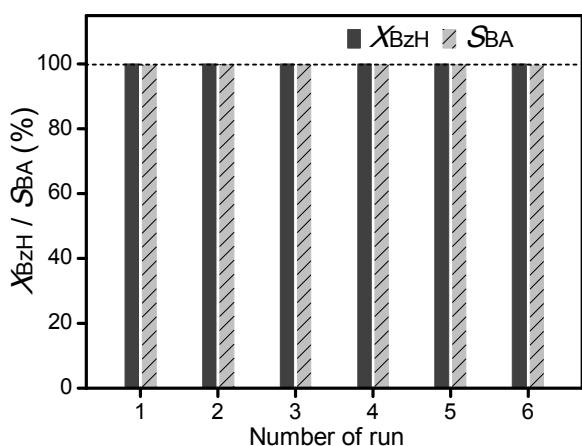


Fig. 4. Reusability of the 0.2Pt/MgAl<sub>2</sub>O<sub>4</sub> catalyst for the hydrogenation of benzaldehyde in ethanol. Reaction conditions: 20.0 mg catalyst, 100  $\mu$ L BAL, 5.0 mL ethanol, 1.0 MPa of H<sub>2</sub>, 60  $^{\circ}$ C, 4 h.

typical impregnation method, the coexistence of multiple Pt species seems to be inevitable, and it is currently impossible to quantify the relative amounts of the species in the mixture. Fortunately, the dispersion of the surface Pt atoms, which are potential active sites accessible to reactants, can be estimated empirically by CO chemisorption experiments, irrespective of whether they are present on the surface of the MgAl<sub>2</sub>O<sub>4</sub> support or as Pt aggregates/crystallites. Accordingly, we obtained the Pt dispersions and calculated the TOFs using the empirical assumption that the stoichiometry of CO adsorption on Pt is equal to 1. This is appropriate for comparison with results reported in the literature that use a similar assumption. However, the detection of bridged carbonyl species suggests that the CO/Pt stoichiometry needs to be corrected by deconvolution of the contribution of the linear and bridged carbonyls using a CO/Pt ratio of 1 or 2, respectively. As shown in Table 4, the ratios of surface Pt with linear (Pt<sub>L</sub>) and bridged (Pt<sub>B</sub>) carbonyl species were calculated to be 90/10 and 44/56 for 0.2Pt/MgAl<sub>2</sub>O<sub>4</sub> and 1Pt/MgAl<sub>2</sub>O<sub>4</sub>, respectively. Accordingly, the Pt dispersions were calibrated to be approximately 100% and 73.9%, respectively. As a result, the corresponding TOFs were determined to be 3430 and 4134 h<sup>-1</sup> at approximately 20% BzH conversion at 60  $^{\circ}$ C. Such amendments to the overall TOFs, however, still do not reflect the intrinsic activity of specific active sites. As we have revealed above, different Pt species present various FTIR

Table 4

Calibrated Pt dispersions and TOFs of various Pt species.

Catalyst	Pt <sub>L</sub> /Pt <sub>B</sub> <sup>a</sup>	Calibrated Pt dispersion <sup>b</sup> (%)	Calibrated TOF <sup>c</sup> (h <sup>-1</sup> )	Averaged TOF of Pt <sub>L</sub> (h <sup>-1</sup> )	Averaged TOF of Pt <sub>B</sub> (h <sup>-1</sup> )
0.2Pt/MgAl <sub>2</sub> O <sub>4</sub>	90/10	~100	3430	3277	4807
1Pt/MgAl <sub>2</sub> O <sub>4</sub>	44/56	73.9	4134	3277	4807

<sup>a</sup> Atom ratio of Pt with linear (Pt<sub>L</sub>) and bridged (Pt<sub>B</sub>) carbonyl species, estimated from  $A_{HF}/2A_{LF}$  in which  $A_{HF}$  and  $A_{LF}$  are the peak area at high and low frequency region as labeled in Fig. 3, respectively.

<sup>b</sup> Recalculated the results of CO chemisorption at 50  $^{\circ}$ C with CO/Pt = 1 and 2 for the fractions of linear and bridged carbonyl, respectively.

<sup>c</sup> Recalculated using the activity of the catalysts at ~20% BzH conversion at 60  $^{\circ}$ C and the calibrated Pt dispersion.

bands for chemisorbed CO owing to the different local coordination environments. In principle, each type of Pt species could be distinguished and quantified by deconvoluting the characteristic band; however, there is a high risk of over-interpreting the FTIR spectra if we try to deconvolute the broad IR bands into many specific bands with slightly different shifts. Here we consider only the relative contributions of Pt<sub>L</sub> and Pt<sub>B</sub> atoms, even though both include several types of Pt species. Thus, the average TOFs of Pt<sub>L</sub> and Pt<sub>B</sub> were calculated to be 3277 and 4807 h<sup>-1</sup>, respectively, without further considering the differences in the detailed structures of the Pt<sub>L</sub> and Pt<sub>B</sub> atoms in the 0.2Pt/MgAl<sub>2</sub>O<sub>4</sub> and 1Pt/MgAl<sub>2</sub>O<sub>4</sub> catalysts. Thus, it can be concluded that the Pt<sub>B</sub> atoms are considerably more active than the Pt<sub>L</sub> atoms. Considering that some of the Pt<sub>L</sub> atoms exist in the Pt crystallites, we can estimate that the activity of the crystallite surface atoms is higher than that of the single atoms on the MgAl<sub>2</sub>O<sub>4</sub> support. The additional ability of the 1Pt/MgAl<sub>2</sub>O<sub>4</sub> catalyst, which is rich in terrace Pt atoms, to hydrogenate BA to TOL suggests that the origin of this increased activity could be the ability to form bridged carbonyl groups. This is in line with the observation that TOL formation usually occurs on well-crystallized nanocatalysts [5,28,29].

#### 4. Conclusions

We have demonstrated that Pt can be readily dispersed as single atoms on an MgAl<sub>2</sub>O<sub>4</sub> spinel support and forms various dispersed Pt species, such as isolated or neighboring single Pt atoms, amorphous aggregates and crystallites, according to the local surface density of the Pt atoms. The single-atom Pt species located directly on the MgAl<sub>2</sub>O<sub>4</sub> spinel surface are highly active in the selective catalytic hydrogenation of BzH to BA over a wide temperature range. The terrace atoms on the Pt crystallites are more active but less selective, and have the ability to further hydrodeoxygenate BA to TOL. These MgAl<sub>2</sub>O<sub>4</sub> spinel-supported Pt single-atom catalysts represent a novel type of catalyst with high stability and selectivity for carbonyl hydrogenation.

#### References

- [1] H. U. Blaser, C. Malan, B. Pugin, F. Spindler, H. Steiner, M. Studer, *Adv. Synth. Catal.*, **2013**, 345, 103–151.
- [2] R. M. Mironenko, O. B. Belskaya, T. I. Gulyaeva, M. V. Trenikhin, A. I. Nizovskii, A. V. Kalinkin, V. I. Bukhtiyarov, A. V. Lavrenov, V. A. Likhoholobov, *Catal. Today*, **2017**, 279, 2–9.
- [3] N. Perret, F. Cardenas-Lizana, M. A. Keane, *Catal. Commun.*, **2011**, 16, 159–164.
- [4] R. Merabti, K. Bachari, D. Halliche, Z. Rassoul, A. Saadi, *React. Kinet. Mech. Catal.*, **2010**, 101, 195–208.
- [5] M. Han, H. L. Zhang, Y. K. Du, P. Yang, Z. W. Deng, *React. Kinet. Mech. Catal.*, **2011**, 102, 393–404.
- [6] R. M. Mironenko, O. B. Belskaya, V. I. Zaikovskii, V. A. Likhoholobov, *Monatsh. Chem.*, **2015**, 146, 923–930.
- [7] R. L. Augustine, *Heterogeneous Catalysis for the Organic Chemist*, Dekker, New York, **1996**.
- [8] G. V. Smith, F. Notheisz, *Heterogeneous Catalysis in Organic Chemistry*, Academic Press, San Diego, **1999**.

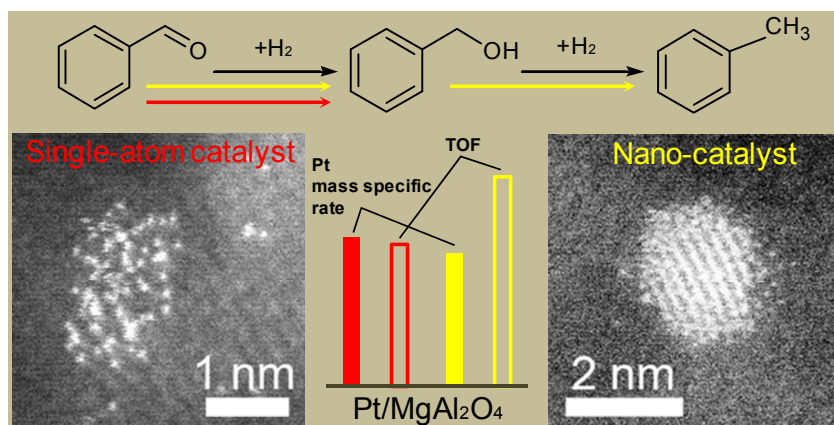
## Graphical Abstract

Chin. J. Catal., 2017, 38: 1613–1620 doi: 10.1016/S1872-2067(17)62815-8

Effect of the degree of dispersion of Pt over MgAl<sub>2</sub>O<sub>4</sub> on the catalytic hydrogenation of benzaldehyde

Feng Yan, Caixian Zhao, Lanhua Yi\*, Jingcai Zhang, Binghui Ge, Tao Zhang, Weizhen Li\*

Xiangtan University; Dalian Institute of Chemical Physics, Chinese Academy of Science; Institute of Physics, Chinese Academy of Science



MgAl<sub>2</sub>O<sub>4</sub>-supported Pt single-atom catalysts are highly active in the selective hydrogenation of benzaldehyde to benzyl alcohol. Pt nano-catalysts are more active but less selective, presumably because of the formation of Pt terraces.

- [9] J. H. Kwak, J. Z. Hu, D. H. Mei, C. W. Yi, D. H. Kim, C. H. F. Peden, L. F. Allard, J. Szanyi, *Science*, **2009**, 325, 1670–1673.
- [10] M. Dhiman, V. Polshettiwar, *J. Mater. Chem. A*, **2016**, 4, 12416–12424.
- [11] W. Z. Li, L. Kovarik, D. H. Mei, M. H. Engelhard, F. Gao, J. Liu, Y. Wang, C. H. F. Peden, *Chem. Mater.*, **2014**, 26, 5475–5481.
- [12] T. Y. Chang, Y. Tanaka, R. Ishikawa, K. Toyoura, K. Matsunaga, Y. Ikuhara, N. Shibata, *Nano Lett.*, **2014**, 14, 134–138.
- [13] M. Yang, S. Li, Y. Wang, J. A. Herron, Y. Xu, L. F. Allard, S. Lee, J. Huang, M. Mavrikakis, M. Flytzani-Stephanopoulos, *Science*, **2014**, 346, 1498–1501.
- [14] B. T. Qiao, A. Q. Wang, X. F. Yang, L. F. Allard, Z. Jiang, Y. T. Cui, J. Y. Liu, J. Li, T. Zhang, *Nat. Chem.*, **2011**, 3, 634–641.
- [15] X. F. Yang, A. Q. Wang, B. T. Qiao, J. Li, J. Y. Liu, T. Zhang, *Acc. Chem. Res.*, **2013**, 46, 1740–1748.
- [16] J. Lin, A. Q. Wang, B. T. Qiao, X. Y. Liu, X. F. Yang, X. D. Wang, J. X. Liang, J. Li, J. Y. Liu, T. Zhang, *J. Am. Chem. Soc.*, **2013**, 135, 15314–15317.
- [17] H. S. Wei, X. Y. Liu, A. Q. Wang, L. L. Zhang, B. T. Qiao, X. F. Yang, Y. Q. Huang, S. Miao, J. Y. Liu, T. Zhang, *Nat. Commun.*, **2014**, 5, 5634.
- [18] X. K. Gu, B. T. Qiao, C. Q. Huang, W. C. Ding, K. J. Sun, E. S. Zhan, T. Zhang, J. Y. Liu, W. X. Li, *ACS Catal.*, **2014**, 4, 3886–3890.
- [19] B. T. Qiao, J. Lin, A. Q. Wang, Y. Chen, T. Zhang, J. Y. Liu, *Chin. J. Catal.*, **2015**, 36, 1505–1511.
- [20] B. T. Qiao, J. X. Liang, A. Q. Wang, J. Y. Liu, T. Zhang, *Chin. J. Catal.*, **2016**, 37, 1580–1587.
- [21] J. Jones, H. F. Xiong, A. T. DeLaRiva, E. J. Peterson, H. Pham, S.R. Challa, G. S. Qi, S. Oh, M. H. Wiebenga, X. I. Pereira Hernandez, Y. Wang, A. K. Datye, *Science*, **2016**, 353, 150–154.
- [22] W. Z. Li, L. Kovarik, D. H. Mei, J. Liu, Y. Wang, C. H. F. Peden, *Nat. Commun.*, **2013**, 4, 2481.
- [23] M. J. Kale, P. Christopher, *ACS Catal.*, **2016**, 6, 5599–5609.
- [24] K. I. Hadjiivanov, G. N. Vayssilov, *Adv. Catal.*, **2002**, 47, 307–511.
- [25] Y. H. Zhou, J. Liu, X. Y. Li, X. L. Pan, X. H. Bao, *J. Nat. Gas Chem.*, **2012**, 21, 241–245.
- [26] Y. K. Du, W. Zhang, X. M. Wang, P. Yang, *Catal. Lett.*, **2006**, 107, 177–183.
- [27] M. A. Vannice, D. Poondi, *J. Catal.*, **1997**, 169, 166–175.
- [28] O. B. Belskaya, R. M. Mironenko, V. A. Likholobov, *Theor. Exp. Chem.*, **2013**, 48, 381–385.
- [29] M. Okamoto, T. Hirao, T. Yamaai, *J. Catal.*, **2010**, 276, 423–428.

Pt在MgAl<sub>2</sub>O<sub>4</sub>载体上的分散程度对催化苯甲醛加氢反应影响鄢 峰<sup>a,b</sup>, 赵才贤<sup>a</sup>, 易兰花<sup>a,\*</sup>, 张景才<sup>b</sup>, 葛炳辉<sup>c</sup>, 张 涛<sup>b</sup>, 李为臻<sup>b,#</sup><sup>a</sup>湘潭大学化学系环境友好化学与应用教育部重点实验室, 湖南湘潭411105<sup>b</sup>中国科学院大连化学物理研究所催化基础国家重点实验室, 辽宁大连116023<sup>c</sup>中国科学院物理研究所北京凝聚态物理国家实验室, 北京100190

**摘要:** 构建催化剂特别是在亚纳米尺度下分散的贵金属催化剂的构效关系是多相催化研究领域中的主要任务之一。我们采用与金属Pt具有强相互作用的MgAl<sub>2</sub>O<sub>4</sub>尖晶石作为载体, 通过简单浸渍法制备了在纳米、亚纳米和单原子尺度上分散的Pt催化剂。首先利用X射线衍射和原子分辨的球差校正电镜, 确定了Pt在MgAl<sub>2</sub>O<sub>4</sub>尖晶石载体表面上随负载量增大逐渐形成孤立的和相邻的单原子Pt, 然后逐渐形成无定形Pt聚集体和小晶粒; 然后利用电感耦合等离子体光谱和CO化学吸附测

定了催化剂中Pt的含量和分散度;进一步通过测定CO在Pt表面吸附的红外光谱,区分了载体表面单原子和金属颗粒表面原子的CO吸附特征结构,并据此对不同结构的Pt原子进行了半定量估算.考察了具有不同Pt分散结构的Pt/MgAl<sub>2</sub>O<sub>4</sub>催化剂的催化苯甲醛选择性加氢能力,发现以载体表面Pt单原子物种为主的催化剂,可在较宽的温度区间内保持较高的部分加氢产物苯甲醇的选择性(60–150 °C, 苯甲醇选择性99.4–97.9%, 甲苯选择性~0.4%),而以Pt纳米颗粒为主的催化剂上苯甲醇选择性降低显著,同时生成较多深度加氢产物甲苯(60–150 °C, 苯甲醇选择性99.0–93.1%, 甲苯选择性0.7–5.0%).此外,我们测定了各催化剂在不同转化率(~20–90%)时催化剂加氢反应的质量比活性和转化频率(TOF),并在较低苯甲醛转化率(~20%)时,估算了不同结构Pt物种对苯甲醛加氢反应的本征活性,发现Pt纳米颗粒表面原子比MgAl<sub>2</sub>O<sub>4</sub>载体表面Pt单原子本征活性更高(4807 h<sup>-1</sup> versus 3277 h<sup>-1</sup>).综上, Pt单原子催化剂具有贵金属原子利用率高,本征活性和加氢选择性高等优点; Pt纳米催化剂表面原子深度加氢能力强,加氢选择性较差,虽本征活性更高,但不足以补偿贵金属原子利用率降低带来的活性损失, Pt质量比活性显著低于单原子催化剂.此外, MgAl<sub>2</sub>O<sub>4</sub>尖晶石负载的单原子Pt催化剂也具有良好的催化反应循环稳定性,是一种较为理想的催化苯甲醛选择性加氢制苯甲醇催化剂.

**关键词:** 铂; 镁铝尖晶石; 单原子催化剂; 选择加氢; 苯甲醛; 苯甲醇

收稿日期: 2017-02-14. 接受日期: 2017-03-15. 出版日期: 2017-09-05.

\*通讯联系人. 电话: (0731)58293719; 传真: (0731)58292477; 电子信箱: yilanhua@xtu.edu.cn

#通讯联系人. 电话: (0411)84379738; 传真: (0411)84685940; 电子信箱: weizhenli@dicp.ac.cn

基金来源: 国家自然科学基金(21403213, 21673226, 21376236, U1462121); 中国科学院“百人计划”; 国家重点研发计划(2016YFA0202801); 中国科学院战略性先导科技专项(XDB17020100); 辽宁省科技厅(2015020086-101); 湖南省自然科学基金(2016JJ2128).

本文的英文电子版由Elsevier出版社在ScienceDirect上出版(<http://www.sciencedirect.com/science/journal/18722067>).